FFP12 2011
Udine 21-23 November 2011

CMB ANISOTROPY COMPUTATIONS USING HYDRA GAS CODE

Màrius Josep Fullana i Alfonso, *Institut de Matemàtica Multidisciplinària, Universitat Politècnica de València, Camí de Vera s/n, 46022 València, e-mail: mfullana@mat.upv.es*
Josep Vicent Arnau i Córdoba, *Departament de Matemàtica Aplicada, Universitat de València, Dr. Moliner 50, 46100 Burjassot, Spain*
Robert J. Thacker, *Department Astronomy & Physics, St. Mary's University, Halifax, Nova Scotia, B3H 3C3 Canada*
Hugh M.P. Couchman, *Department of Physics and Astronomy, McMaster University, 1280 Main St. West, Hamilton, Ontario, L8S 4M1, Canada*
Diego P. Sáez Milán, *Departament d'Astronomia i Astrofísica, Universitat de València, Dr. Moliner 50, 46100 Burjassot, Spain*

Abstract
From FFP6 to FFP11, we presented the advances in our Cosmic Microwave Background (CMB) anisotropy computations using N-body Hydra Codes. For such computations, codes without baryons were used: First sequential versions and afterwards parallel ones. With both of them we computed the weak lensing and the Rees-Sciama contributions to the CMB angular power spectrum. Using our numerical techniques, we reported a lensing effect higher than that estimated in previous papers (for very small angular scales). Our CMB computations require less interpolations and approximations than other approaches. This could explain part of our excess of power in lensing computations. Our higher time and angular resolutions could also contribute to this excess. Here, recent advances on previous computations are presented. Computations with baryons have been started. These calculations allow us to compute the Sunyaev-Zel'dovich contribution to the CMB angular power spectrum. We are also trying to compute the three effects -weak lensing, Rees-Sciama and Sunyaev-Zel'dovich- at the same time, with the essential aim of seeing how their power spectra couple among them.

1. Introduction
Rough estimates of CMB anisotropies performed with PM codes may be found, e.g., in (Fullana 2004) and (Puchades 2006). These calculations were improved by using AP3M codes with more resolution. We first used a Hydra AP3M sequential code (Fullana 2008), which was modified to move the CMB photons through the AP3M n-body simulations. Only dark matter was taken into account to evolve structures and compute Rees-Sciama (RS) and weak lensing (WL) CMB anisotropies. Afterwards, a Hydra AP3M parallel code was used to do the same estimates (RS and WL effects) with more resolution and bigger boxes (Fullana 2010a). Again only dark matter was taken into account in the evolution of structure. Now, we are moving CMB photons along the simulation boxes of a Hydra AP3M parallel code with baryons. The RS and WL CMB anisotropies have been calculated again --with similar boxes and resolution-- to compare with previous results obtained without baryons. The calculation of the Sunyaev-Zel'dovich (SZ) effect is being performed by using appropriate resolutions and our ray-tracing techniques, which were designed to move CMB photons thorough the simulated boxes while the code is running. The peculiar gravitational potential, its gradients, the electron number density, and other necessary quantities are calculated and used at every time step of the Hydra simulation. More details about previous work may be found in other FFP Proceedings (Fullana 2004, 2007, 2008 and 2010b).

2. Map Construction
WL deflections are given by the following formula:

$$\delta = -2 \int W(\lambda)\, \nabla_{\perp}\phi \; d\lambda, \qquad (1)$$

where $\nabla_{\perp}\phi$ is the transverse gradient of the peculiar gravitational potential, $W(\lambda) = (\lambda_{em}-\lambda)/\lambda$, *and*

$$\lambda(a) = H_0^{-1} \int (\Omega_m b + \Omega_\Lambda b^4)^{-1/2}\, db, \qquad (2)$$

H_0, Ω_m, and Ω_Λ being the Hubble constant, and the density parameters of matter and vacuum, respectively. By using these formulas, the temperature contrasts $\Delta T/T$, and the C_l coefficients due to WL may be calculated (Fullana 2010a). The integral (2) is to be done in the interval [a,1].
The RS, thermal SZ, and kinetic SZ temperature contrasts are given by the expressions

$$\Delta T/T = 2 \int \partial\phi/\partial t \, dt \,, \quad (3)$$

$$\Delta T/T = (-2\sigma_T \, k / m_e c^2) \int n_e \, (T_e - T_{CMB}) \, dl \,, \quad (4)$$

and

$$\Delta T/T = - (\sigma_T / c) \int v_r \, n_e \, dl \,, \quad (5)$$

respectively, where n_e, T_e, T_{CMB}, v_r, σ_T, k, m_e and c are the electron number density, the electron and CMB temperature, the radial component of the peculiar velocity, the Thompson cross section, the Boltzmann constant, the electron mass and the speed of light, respectively. Integrals (1), (3), (4) and (5) are to be calculated along the background null geodesics.

3. Evaluating variables to perform integrations

In order to compute the integrals of eqs. 1, 3, 4 and 5, we proceed as follows:

1) Select the propagation directions of the CMB photons (ray-tracing).
2) Assume the Born approximation, and use the photon step distance, Δ_{ps}, to determine all the evaluation positions on the background null geodesics, from the initial to the final redshift. Then, localize each of these positions inside one of the simulation boxes.
3) Associate a test particle to each evaluation position. Times are obtained from the null geodesic equations in the background.
4) At each time step of the N-body simulation (while it is running), determine which test particles require evaluations (peculiar potential, forces, temperature, and so on), and evaluate by using the long-range FFT component and short-range PP correction given by the Hydra algorithm (if it is necessary). The SZ effect, eqs. 4 and 5, requires the number density and temperature of electrons on the test particle position, which may be estimated from the outputs of the Hydra code. The RS effect given by eq. 3 uses the peculiar gravitational potential and, finally, the WL effect is obtained from the transverse component of the peculiar gravitational force.
5) Avoid contributions to the peculiar gravitational potential due to scales larger than 42 $h^{-1}Mpc$, it may be done by removing the signal, in Fourier space, for wavenumbers $k < 0.15 \, h \, Mpc^{-1}$. The use of this cutoff in WL and RS calculations is justified in next section.
6) If the evaluation time for a test particle lies between the two times defining a time step of the simulation, use linear interpolation between these two times to do the required evaluation.

4. Description of the simulations

Simulations are done in the framework of the concordance model with the following parameters: reduced Hubble constant, h=0.7; baryon, dark matter, and dark energy density parameters Ω_b= 0.046, Ω_d = 0.233 and Ω_Λ = 0.721, respectively; optical depth for reionization, τ = 0.084, and matter power spectrum normalisation parameter, σ_8 = 0.817. No tensor modes are considered. It has been verified that the hydra code produces the same structure without CMB photons (original tested version) and with them. The CMB photons are moved through the simulation box along specially chosen oblique paths and the boxes are not moved at all. In this way, the periodicity inside the box volume ensures that there are no discontinuities in the fields where photons cross from box to box. We take care to ensure that, for the chosen paths, periodicity effects become negligible. To minimize these effects, the photons must cross consecutive boxes through statistically independent regions, which require: (i) *preferred directions* leading to large enough distances between these regions and, (ii) a suitable cutoff avoiding large scale spatial correlations ($k < 0.15 \, h \, Mpc^{-1}$) between the above distant regions. For the preferred directions (see Antón 2005, Sáez 2006 and Fullana 2008), and box sizes of L_{box} = 256 $h^{-1}Mpc$, it can be easily verified that the CMB photons can travel from z=6 to z=0 (~ 5900 $h^{-1}Mpc$) through different uncorrelated regions (without repetitions) located in successive simulation boxes. The total number of crossed boxes is *close to 20*. Our squared CMB maps are uniformly pixelised by choosing a certain number of pixels, N_{pix}, per edge. The angular resolution is then $\Delta_{ang} = \Phi_{map} / N_{pix}$ (Φ_{map} being the angular size of the map side). A preferred direction points toward the centre of any squared map. Since the maps are small, the directions of all the pixels are close to the central one and, consequently, they are also preferred directions. Therefore, lens deviations can be calculated for each pixel, with no

significant periodic effects across the full map. For greater box sizes, the situation is better (see Fullana 2010a).
This is notably different from other approaches using random translations and rotations (Carbone 2008) of the simulation box which, unavoidably, lead to discontinuities at crossing points between adjoining boxes.
Let us now list the parameters involved in our ray-tracing procedure: a number of directions, N_{dir}, per edge of the squared CMB map (one per pixel, $N_{dir} = N_{pix}$); an initial redshift, z_{in}, a photon step, Δ_{ps}, to perform the integrals in eqs.1, 3, 4 & 5; and the angles θ and φ defining the preferred direction. A simulation (with CMB photons) is characterized by the parameters and initial conditions required by the Hydra simulations (without CMB photons) together with the parameters of the ray-tracing.
For computations without baryons (WL and RS effects), the simulation parameters chosen in this paper are: $L_{box} = 512\ h^{-1}Mpc$, number of particles $N_p = 512^3$, number of cells $N_c = 1024^3$, softening $S_p = 12\ h^{-1}kpc$, $N_{dir} = 512$, $z_{in} = 6$ and $\Delta_{ps} = 25\ h^{-1}kpc$. The angular resolution of these simulations is $\Delta_{ang} \simeq 0.59'$ ($l \simeq 18{,}600$). The map size is ~ 5º × 5º. The effective resolution is E_{res} ~ 60 $h^{-1}kpc$. N-body simulations of this type were presented in (Fullana 2010a). In our new simulations with baryons, the same parameters, except $N_p = 2 \times 512^3$, are first chosen to facilitate some necessary comparisons. Nevertheless, further applications of our simulations with baryons require more resolution, and the above simulation parameters must be changed (see below).

5. Previous results and perspectives

N-body simulations as those described in section 4 were previously used (Fullana 2010a) to estimate the angular power spectrum of the WL effect. The signal in the range $4200 < l < 7000$ was $2.0 \pm 0.4\ \mu K$, which is ~ 1.4 μK higher than that found elsewhere (Das 2008). Our direct estimate of the potential gradients at photon positions --using the same PP corrections as for dark matter particles-- seems to be the main origin of the difference between our results and other researches based on projection planes and grid interpolations. These differences appear only at large $l > 2000$. Moreover, our method employs extremely fine time resolution (that of the AP3M simulation) and also a very good angular resolution.
Our code was run for a wide range of the parameters involved in the N-body simulations and in the ray-tracing procedure (see section 4), in this way, it was studied how the resulting angular power spectra depend on all these parameters. Since the dependence is weak, results appear to be robust (Fullana 2010a), at least in the l-interval (4200,7000).
On small scales, baryons do not follow the dark matter distribution. Therefore, while we have attempted to be as accurate as possible in our dark matter simulations (without baryons), we are probing scales where contributions from baryons are beginning to become significant. A study of the impact of baryons can be found in (Jing 2006). We are beginning to conduct simulations with baryons and feedback processes both to identify its impact on WL and RS signals, and also to systematically evaluate the combined impact of the SZ, WL, and RS effects.
The SZ effect dominates on total lensing for $4200 < l < 7000$. In (Fullana 2010a), we discussed the implications of our estimates taking into account the CBI observations (Bond 2005) and the BIMA measurements (Dawson 2006), which were the most significant anisotropy measurements (at very small angular scales) when that paper was written. The discussion took into account that the SZ power scales as $\sigma_8^{3.5}$. Then, the SZ effect associated to the σ_8 value measured by WMAP was too small to explain the high power observed by BIMA for the small angular scales under consideration. In that situation, our excess of WL power seemed to be an appropriate though small excess contributing to the explanation of the large BIMA power.
Afterwards, new data for small angular scale measurements of the CMB anisotropy changed the situation. Observations performed with the ACT (Fowler 2010) and the SPT (Lueker 2010) telescopes indicated that, for large l-values, the CMB power is much smaller than that previously reported by CBI and BIMA experiments. The new situation was discussed in (Fullana 2010b). For example, in the l-interval (5000, 6000), the ACT power is between ~ 40 μK^2 and ~ 50 μK^2 (see Fig. 4 of Fowler 2010). This power might be explained by the coupling of SZ, foreground radiation of Dusty Star Forming Galaxies (DSFG), plus almost negligible lensing (that predicted by previous simulations); however, our large WL effect of ~ 6 μK^2 might complicate the explanation of the small ACT power. Anyway, our WL power may be compatible with the small ACT and SPT powers taking

into account that (i) there are uncertainties in the radiation from DSFG, (2) the SZ effect should be studied in more detail, e.g., by using our ray-tracing procedure, and (3) the coupling between SZ, WL and RS effects might lead to a total power different from the simple addition of powers. Of course, the observed power must be explained by the correct coupling of WL, SZ, RS and DSFG contributions. It is worthwhile to emphasize that the WL and SZ effects are essentially produced by the same structure distributions (galaxy clusters and sub-structures involving dark matter and baryons) and, consequently, these effects must be strongly correlated. This implies that the spectra of these two effects must be superposed in an unknown way (not merely added). In practice, this superposition might be analyzed in detail with ray-tracing through hydra simulations including both baryons and dark matter.

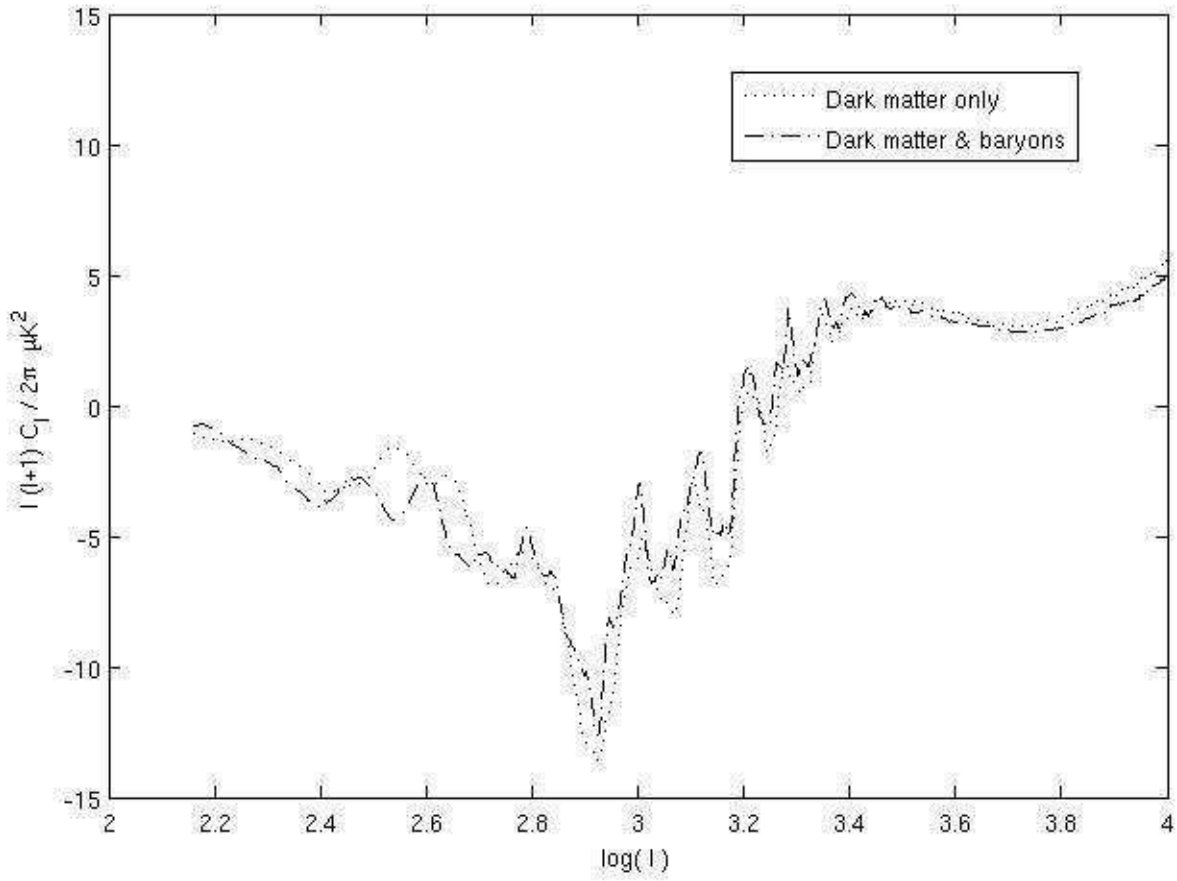

Figure 1: Comparison of WL spectra corresponding to Hydra simulations with and without baryons. Parameters defining these simulations are given in the last paragraph of section 4.

6. Current work and projects

A version of a certain Hydra code with baryons has been modified to include CMB photons. Some subroutines and the computational load allocation configuration of the initial code have been remodelled. The resulting code has been tested. One of the most powerful tests is based on the comparison of the WL and RS power spectra obtained by using simulations with and without baryons (for the parameters given in section 4). Results of both types of simulations are expected to be very similar. Small differences might appear as a result of various facts. Let us now list some of them: (i) simulations without baryons have been performed with a SGI Altix 3700 computer and a Pathscale compiler, and the other type of simulations with an SGI Altix UV 1000 computer and an Intel compiler, (ii) the initial Hydra codes we have modified --introducing CMB photons-- exhibited some technical differences, and (iii) it is known that the presence of baryons alter the WL spectrum at very small angular scales (Jing 2006). The WL angular power spectra obtained with and without baryons are compared in fig. 1, where the spectrum with baryons (point-dashed line)

appears to be rather similar to that corresponding to dark matter only (dotted line). Although the slight differences are being studied yet, they strongly suggest that codes with and without baryons are working properly and also that new simulations with more resolution seem to be necessary to estimate the physical effect produced by the presence of baryons and to compare with (Jing 2006). We think that simulations based on the following parameters would be appropriate: $L_{box} = 200\ h^{-1}$ *Mpc*, $N_p = 2 \times 640^3$, $N_c = 1280^3$, $N_{dir} = 512$, $z_{in} = 6$, and S_p and Δ_{ps} to be adjusted to our new computational procedure. The angular resolution of these simulations is $\Delta_{ang} \simeq 0.24'$, and the map size is ~ 2º × 2º. These simulations would be also useful to develop our main projects: (1) the estimate of the SZ effect by using our ray-tracing procedure, (2) the calculation of the total anisotropy produced by the RS, WL, and SZ effects, whose superposition may be nonlinear, and (3) the comparison of the resulting total anisotropy with recent observations at very small angular scales (Fowler 2010, Lueker 2010).

Acknowledgments

This work has been partially supported by the Spanish Ministerio de Educación y Ciencia, MEC-FEDER project FIS2009-07705

References

Fullana, M J and Sáez D (2004) Making Maps of the Rees-Sciama Effect in Proceedings of FFP6, Udine

Puchades N, Fullana M J, Arnau J V and Sáez D (2006) On the Rees-Sciama Effect: Maps and Statistics, MNRAS (370), 1849-1858

Fullana M J, Arnau J V and Sáez D (2008) Weak Lensing on the CMB: Estimations Based on AP3M Simulations in Proceedings of FFP9, Udine

Fullana M J, Arnau J V, Thacker R J, Couchman H M P and Sáez D (2010a) Estimating small angular scale CMB anisotropy with high resolution N-body simulations: weak lensing, ApJ, (712), 367-379

Fullana, M J and Sáez D (2007) Status of CMB Radiation in AIP Conference Proceedings (905) of FFP9, Sidhart B, Alfonso-Faus A and Fullana M J eds., Madrid, 13-22

Fullana M J, Arnau J V, Thacker R J, Couchman H M P and Sáez D (2010b) Recent Observations on CMB at high multipoles and AP3M computations at such scales in Proceedings of FFP11, Paris, 2010, in press

Antón L, Cerdá-Durán, V, Quilis, V and Sáez D (2005) Cosmic Microwave Background Maps Lensed by Cosmological Structures: Simulations and Statistical Analysis, ApJ (628), 1-13

Sáez D, Puchades N, Fullana M J and Arnau J V (2006) Ray-Tracing through N-body simulations and CMB anisotropy estimations} in Proceedings of CMB and Physics of the Early Universe, Ischia, 58-62

Carbone C, Springel V, Baccigalupi, C, Baretelmann, M and Matarrese, S (2008) Full-sky maps for gravitational lensing of the cosmic microwave background MNRAS (388), 1618-1626

Das S and Bode P (2008) A Large Sky Simulation of the Gravitational Lens- ing of the Cosmic Microwave Background. ApJ (682), 1–13

Jing Y P, Zhang P, Lin W P, Gao L and Springel V (2006) The Influence of Baryons on the Clustering of Matter and Weak-Lensing Surveys, ApJ (640), L119-L122

Bond J R et al (2005) The Sunyaev-Zel'dovich effect in CMB-calibrated theories applied to the Cosmic Background Imager anisotropy power at l > 2000, ApJ (626), 12-30

Dawson K S, Holzapfel W L, Carlstrom J E, Joy M and LaRoque S J (2006) Final Results from the BIMA CMB Anisotropy Survey and Search for a Signature of the Sunyaev-Zel'dovich Effect, ApJ (647), 13-24

Fowler J W et al (2010) The Atacama Cosmology Telescope: A Measurement of the 600< ell <8000 Cosmic Microwave Background Power Spectrum at 148 GHz, ApJ (722), 1148-1161

Lueker M et al (2010) Measurements of Secondary Cosmic Microwave Background Anisotropies with the South Pole Telescope, ApJ (719), 1045-1066